Segregation of Cast Medium Mn Steels

Mujeeb H. Shaik
Western Michigan University, Kalamazoo, Michigan, USA

Robert B. Tuttle
Western Michigan University, Kalamazoo, Michigan, USA

ABSTRACT

Quenching and partitioning steels have attained a significant amount of research interest in the past five years. These steels represent a new alloying and heat treatment strategy. Furthermore, they have the potential to provide new market opportunities for steel castings. Many researchers include a homogenization step in the heat treatment to reduce the effect of segregation. However, little data have been presented in the open literature showing such segregation. The work in this paper examines macro and microsegregation in a Y-block casting. Spectrometry of the casting and scanning electron microscopy/energy dispersive X-ray spectroscopy (SEM/EDS) analysis were conducted to characterize the amount of segregation and determine the need for a homogenizing heat treatment. Little segregation was found, which indicates a homogenizing step is unnecessary in the size range of the Y-block used.

Keywords: quench and partition, Q&P, medium manganese steel, macrosegregation, microsegregation

INTRODUCTION

Quenching and partitioning (Q&P) is a relatively new heat treatment process that has emerged as a promising alternative to conventional methods like quenching and tempering. This heat treatment process produces high strength steels with good ductility, which is based on transformation induced plasticity (TRIP). The traditional heat treatment processes for steel, such as quenching and tempering (Q&T), involved rapid cooling followed by reheating to achieve desired properties. In conventional steels, high strength is achieved but ductility is sacrificed.

The Q&P steels have been targeted for Body-in-White (BiW) applications in the automotive industry. Thus, these steels have been designed for sheet metal applications. However, there is significant opportunity in using these alloys for steel castings in the trucking, defense, and aerospace industries. The higher strength and ductility of these alloys would provide weight reduction opportunities that would reduce costs and environmental impact.

There is a large difference in the effect of the Q&P heat treatment on material properties compared to conventional quenching and tempering (Q&T). The Q&P heat treatment produces a different balance between strength and ductility. The Q&P steel has better toughness and impact resistance than Q&T due to the presence of martensite and retained austenite. Most of the property differences are due to the presence of retained austenite which provides the higher ductility without compromising the strength.

There is a large difference in mechanical properties of Q&P and Q&T treated steels. The work by Wendler et al.[1] provides an example of the mechanical properties possible. These authors experimented with a Fe-15Cr-3Ni-3Mn-0.5Si-0.12N-0.16C alloy which had a yield strength (YS) of 1050 MPa, ultimate tensile strength (UTS) over 1550 MPa, and a percent elongation of 22%.[1] On the other hand, a hot rolled 4140[2] Q&T steel has a YS of 1570 MPa, UTS of 1720 MPa, and a percent elongation of 11.5%. Thus, the properties of a Q&P treated steel can be similar to that of a Q&T steel, but with double the elongation. The higher elongation provides a tougher alloy overall. This trend is shown in other studies as well.[3–11]

The Q&P process is schematically shown in Figure 1, and can be divided into three major steps.[12]

1. The first step is to heat the steel to the austenization temperature (AT).
2. The second step is quenching to the quench temperature (QT) which is between martensite start (M_s) and martensite finish (M_f) temperatures to form the desired amount of supersaturated martensite and untransformed austenite.
3. In the third step, the steel is heated to the partitioning temperature (PT) and held there for a predetermined amount of time. This causes the retained austenite to enrich with carbon through the partitioning of carbon from the carbon-supersaturated martensite. After partitioning, the steel is cooled to room temperature.

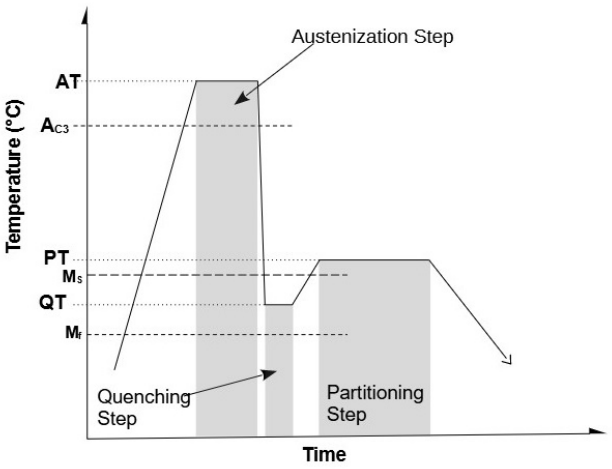

Figure 1. A schematic illustration of the Q&P process.

A key part of the Q&P process is the constrained paraequilibrium (CPE) that occurs during the partitioning stage. Speer developed a model to address carbon partitioning from as-quenched martensite into austenite, under conditions where competing reactions such as bainite, cementite, or transition carbide precipitation are suppressed.[13] In the absence of carbide formation, the CPE condition can be calculated based on straightforward thermodynamic and mass balance constraints.[13] CPE is essentially defined by one thermodynamic requirement, and one key mass balance constraint. First, carbon diffusion occurs when the chemical potential of carbon is equal in ferrite and austenite.[13] Ignoring the effects of alloying on carbon activity, this requirement may be represented using the results of Lobo and Geiger for the Fe-C binary system as follows:[13–16]

$$^{4}X_C^{\gamma} = X_C^{\alpha}.e^{\frac{76{,}789-43.8T-(169{,}105-120.4T)X_C^{\gamma}}{RT}} \quad \textbf{Eqn. 1}$$

Where: X_C^{γ} and X_C^{α} represent the mole fractions of carbon in ferrite and austenite. The relevant thermodynamics are embedded in Equation 1.[13,16]

Speer predicted the martensite start (M_s) temperatures and martensite fraction (f_m) by using Equations 2 and 3. Equation 3 was used to predict the Ms of the steel.

$$Ms(^{\circ}C) = 499 - 317(\%C) - 33(\%Mn) - 28(\%Cr) - 17(\%Ni) - 11(\%Si) - 11(\%Mo) - 11(\%W) \quad \textbf{Eqn. 2}$$

The martensite fraction (f_m) was predicted by using the Koistinen–Marburger Relationship, which relates the degree of undercooling below the Ms to the amount of martensite formed (Equation 3)

$$f_m = 1 - e^{-1.1x10^{-2}(\Delta T)} \quad \textbf{Eqn. 3}$$

Where: f_m is the volume fraction of the martensite and ΔT is the temperature difference between the Ms and the quench temperature. Based on this theory, Speer proposed the quench and partition process.[13] The Q&P process is an approach designed to generate a microstructure with a combination of martensite and controlled amounts of retained austenite. In the Q&P process, the carbon supersaturation of the quenched martensite is used to stabilize the untransformed austenite. The stabilized retained austenite is then available to transform to additional martensite during plastic deformation, which provides additional strength and ductility. This transformation due to deformation is called transformation induced plasticity (TRIP). The volume change associated with the austenite to martensite transformation leads to plastic deformation in the material.

While significant amounts of research have been conducted on the microstructure-property relationships, less has been done on studying the segregation. Many researchers report doing a 1000–1200C (18322192F) homogenizing step prior to the Q&P process and state it is to reduce segregation. However, none provides evidence of this segregation issue.[3,10,17,18] Previous authors have not provided enough information about sampling. Some of the previous work might have taken samples from slabs, which are quite thicker sections. There is no evidence of where the samples originated.

Wang et al. conducted one of the few studies on segregation in medium manganese Q&P steels.[11] They found a segregation band within their specimen where Si and Mn were higher. The highest level of segregation contained 4.7 wt.% Mn and 2.1 wt.% Si, 2.7 wt.% and 0.6 wt.% higher than the overall concentration, respectively.[11] The highest level of segregation was contained in the mid thickness of the 1.4mm thickness specimen.[11] This shows that the Mn was not distributed homogenously. The root cause of Mn segregation was its rejection into the interdendritic liquid during solidification and also due to the slow kinetics of Mn diffusion, permanent elimination of Mn gradients can only be achieved by long high-temperature homogenization treatments.[19]

The use of a homogenizing heat treatment for the Q&P process significantly impacts the cost of the process. This paper covers work conducted to examine the segregation more closely in medium-Mn steels. Two types of analysis were performed to understand the segregation (macrosegregation and microsegregation analysis) to determine alloying element distribution at the macro and micro levels. These two examinations and their results provide guidance on the need for a homogenizing step in these steels.

EXPERIMENTAL PROCEDURE

A 25.4 mm thick Y-block was used in this experiment to study segregation (Figure 2). Molds were made from a resin-bonded silica sand. The sand had an AFS Grain Fineness Number (GFN) of 55, and 2 wt. % phenolic nobake resin. The two-part resin system was mixed with the sand using an industrial mixer and manually compacted into the pattern box. Three molds per heat were poured; however, only one was used for this study.

Twenty-three-kilogram heats were melted in a 3 kHz induction furnace under an air atmosphere in a high alumina crucible. Two different alloys were examined to understand their segregation behavior. These were designated QP1 and QP2 (Table 1). The initial charge consisted of 1010 scrap. Once the melt heated to 1650C (3002F), FeSi, electrolytic manganese, and graphite were added. For QP1, aluminum shot was also added at this stage. The melt was tapped into a magnesia fiber refractory lined ladle at 1740C (3164F). The castings were poured at 1620C (2948F) and allowed to cool for thirty minutes before shakeout occurred. The castings continued to cool to room temperature overnight.

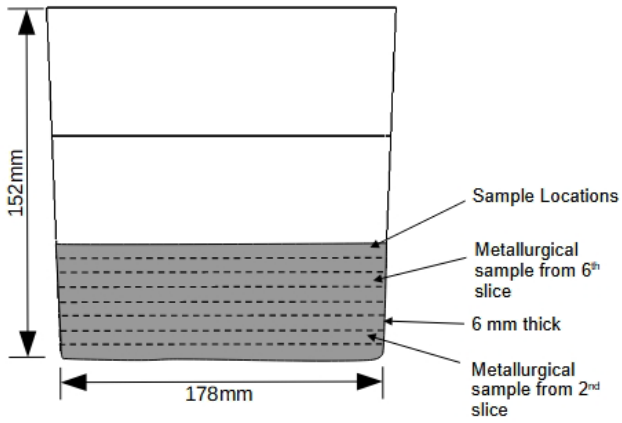

Figure 2. The Y-block casting and slice locations.

Table 1. Chemical Composition for Each Heat (wt. %)

Alloy	*C*	*Si*	*Mn*	*S*	*Cr*	*Al*
QP1	0.25	1.7	3.4	0.011	0.035	0.03
QP2	0.27	1.9	2.1	0.014	0.032	Nil

Figures 3 and 4 show the TTT diagrams for QP1 and QP2 alloy respectively. The M_s and M_f temperatures are indicated in the TTT diagram. These diagrams were calculated using ThermoCalc© with the TCFE V12 database.

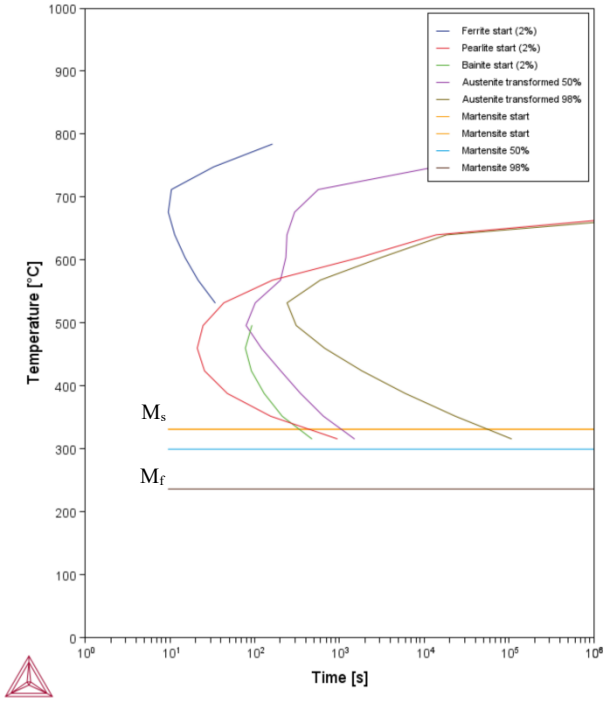

Figure 3. The TTT diagram of QP1.

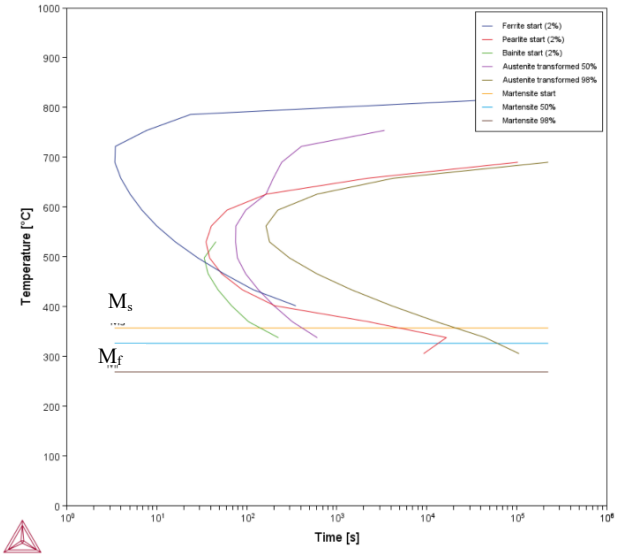

Figure 4. The TTT diagram of QP2 alloy.

For macrosegregation, a vertical bandsaw sectioned the Y-block into eight, 6 mm thick slices. The slices began from the bottom of the Y-block and proceeded until a total depth of 50.8 mm. This final location was selected based on microporosity predictions from solidification simulation performed in Magmasoft.© Above this point, there were significant levels of microporosity, and shrinkage predicted. These pores would interfere with the optical emission spectroscopy (OES). Each slice was designated with a heat letter and number sequence from 1 to 8.

To measure segregation, OES was conducted on all eight slices. Measurements were made at the center of each slice and approximately 25.4 mm from the edge of the slice (Figure 5) and also measured at the outer edge of the slice (Figure 5). Three burns were made at each location with the middle one centered on the dimension indicated. A Hitachi Foundrymaster© was employed for this analysis. Prior to burning, each sample was ground using a 60-grit zirconia sanding belt. The sample number was used to map back to a depth into the Y-Block from the bottom.

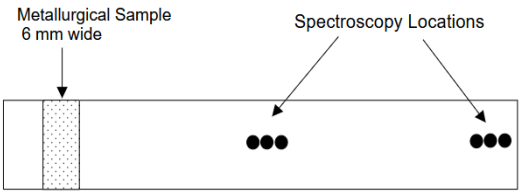

Figure 5. The spectroscopy and microstructure sample locations from Slices 2 and 6 of each heat.

After spectroscopy, Slices 2 and 6 were cut into 6 mm wide metallurgical samples located approximately 25.4 mm from the unburned side of the slice for optical microscopy and scanning electron microscopy (Figure 5). The first cut was with a bandsaw and the second was made with a low-speed diamond saw. Next the samples were mounted in a copper-based conductive mounting compound. This was done to eliminate the carbon coating from the SEM sample. The samples are marked after mounting by heat letter and slice no. of the sample for traceability. The samples were ground using 320, 400, 600, 800, and then 1200 grit SiC sandpaper. After grinding, polishing was accomplished with a 1µm polycrystalline diamond followed by a 0.05 µm alumina slurry. The samples were etched with 3% Nital for 10-15s to reveal the microstructure. Optical microscopy images were captured.

A JEOL JSM-IT200 SEM with a silicon drift detector EDS was employed to analyze the microsegregation within each metallurgical sample. An accelerating voltage of 20 kV and 10 mm working distance were employed.

RESULTS AND DISCUSSION

MACROSEGREGATION

Optical emission spectrometer analysis was done to quantify macrosegregation profiles in the Y-block castings. Figure 6 represents the experimentally measured QP1 composition profiles of carbon with uniform segregation throughout the macrosegregation path. The highest and lowest contents were observed at 44.45 mm with 0.27 wt.% C and 12.7 mm with 0.25 wt. % C respectively. Hence no significance segregation was found. The QP2 has the same amount of carbon content as QP 1 and also no significant difference in distribution was observed (Figure 7). The uniform distribution of carbon is necessary for a microstructure with uniform properties. Regions with higher carbon content may exhibit increased hardness and strength but reduced ductility.

Figure 6 depicts the distribution of manganese in QP1. The QP1 is a medium-Mn alloy with the 3.4 wt. % of Mn. The highest concentration of Mn was observed at the distance of 31.75 mm which was in the center with 3.42 wt. % and lowest concentration was at the distance of 38.1 mm which is in the center with 3.32 wt. %. The QP2 alloy had a similar manganese segregation pattern (Figure 7). In both alloys, the difference between the outside and center locations at each level were similar (Figures 6 and 7). The uniform manganese content indicates the cooling rates were sufficient to create a uniform distribution. This uniform distribution will also ensure a homogenous microstructure upon heat treatment.

Figures 6 and 7 also indicate the concentration of silicon content in the QP1 and QP2 alloy. It was observed that little segregation occurred between the center or outer portions of the Y-block at all levels.

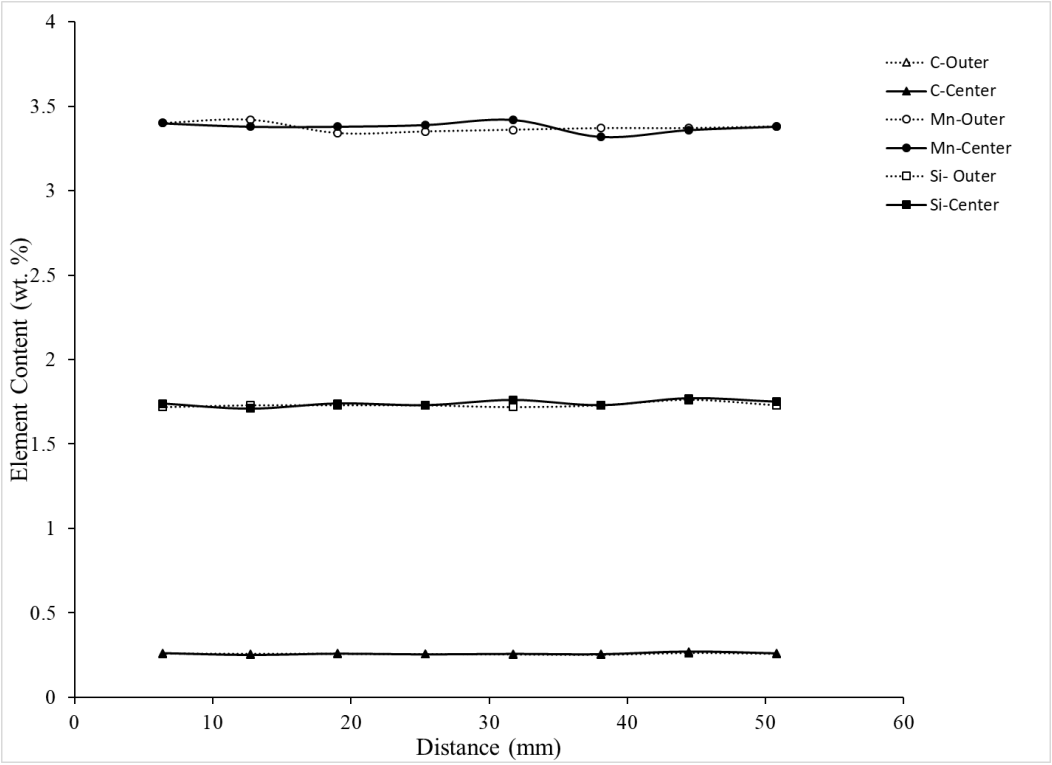

Figure 6. The C, Mn, and Si content for QP1.

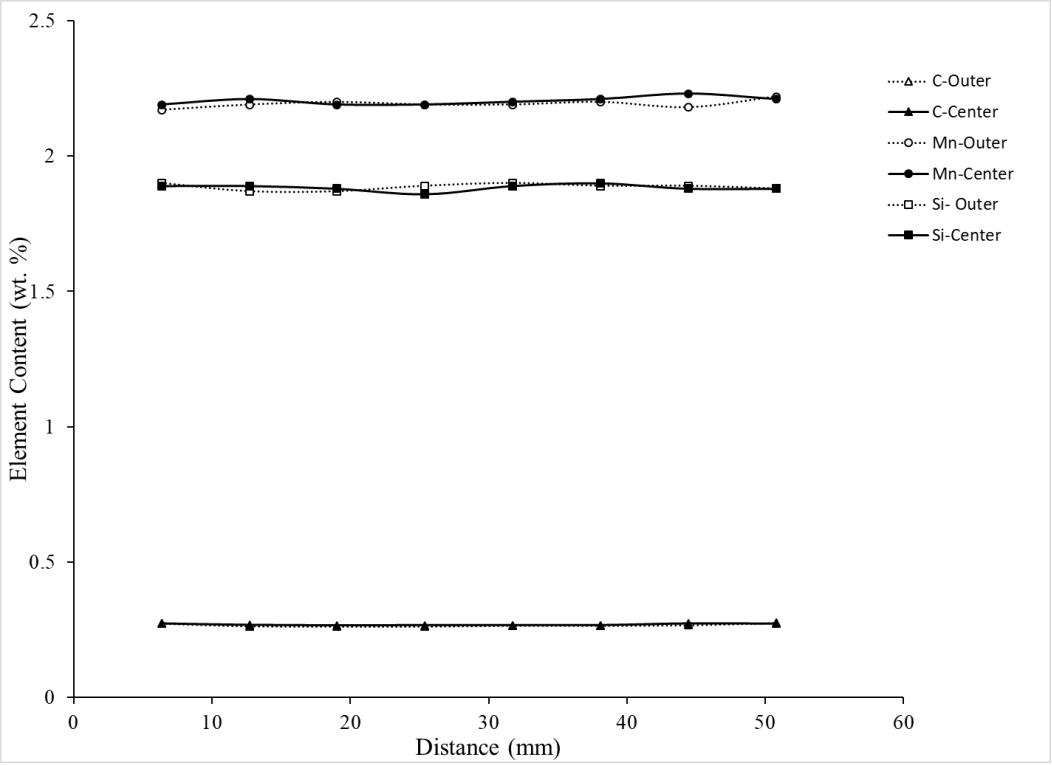

Figure 7. The C, Mn, and Si content for QP2.

MICROSTRUCTURE

For both alloys, samples taken 12 mm and 36 mm from the bottom were examined. There were no significant differences. Figure 8 shows the cooling rates predicted in the simulation, they tend to be similar at all the locations where metallurgical samples were taken. Thus, only the data from the 12 mm location are presented. This lack of difference agrees with the alloy composition data presented in the previous section and confirms little macrosegregation within the Y-block.

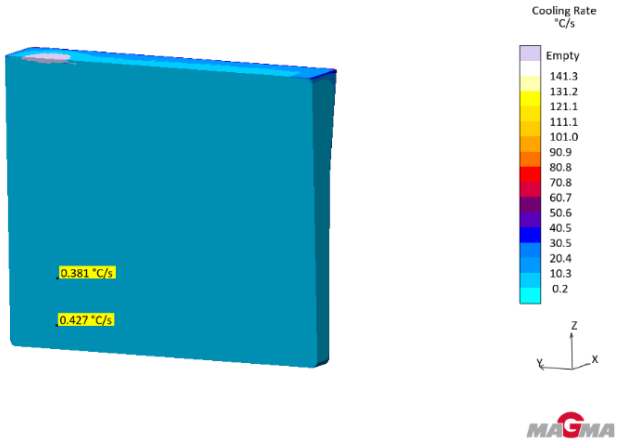

Figure 8. The cooling rates at 12mm and 36mm locations.

Examination of the microstructure for QP1 indicates it was mostly martensite, with small amounts of retained austenite and ferrite (Figure 9). The expected microstructure was ferrite due to low carbon content; the primary expected phase was austenite. Austenite was expected due to the high amounts manganese in this alloy stabilizing it at room temperature. There is no significant composition banding observed in the microstructure. Significant banding in a microstructure can be challenging because it can result in nonuniform properties across the material. Similarly, QP2 also contained large amounts of martensite, but also high levels of austenite (Figure 10).

The formation of martensite was an unexpected occurrence. The authors had expected a ferritic microstructure. It may be due to the early shakeout employed in this work. After the casting was poured, it cooled for 30 minutes and then was shook out. The rapid cooling following shakeout resulted in the formation of martensite, but the transformation was not complete. Despite the shakeout time being common for the Y-block casting in this lab, the high M_s temperatures (~350C/662F) and M_f (~200C/392F) of these alloys enabled the formation of martensite.[4,20] A longer wait time prior to shakeout might prevent this structure from forming in the as-cast condition.

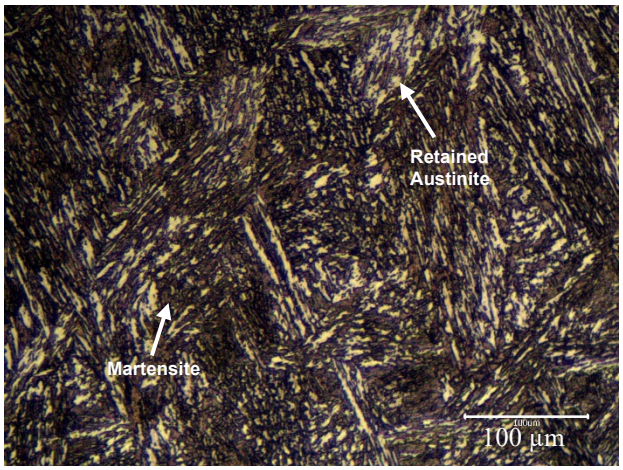

Figure 9. The martensitic microstructure of QP1.

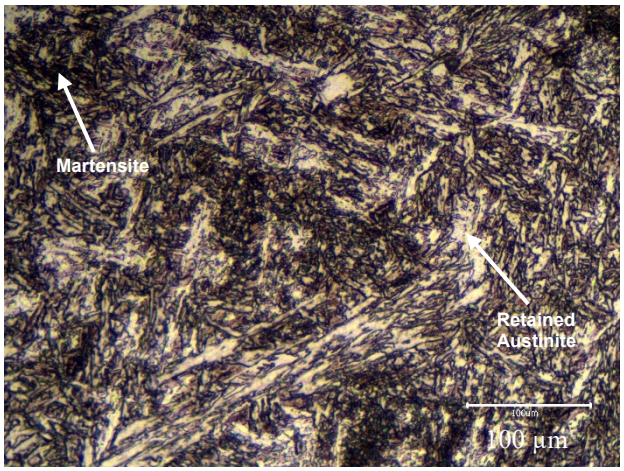

Figure 10. The martensitic and retained austenite microstructure of QP2.

MICROSEGREGATION

Microsegregation is the variation in composition over a very small scale. Typically, the length scale equals the distance between dendrites and dendrite arms in the steel. The microstructure was assessed through EDS analysis, and the results indicate that there is no significant segregation at the micro-level in either QP1 or QP2 (Figures 13 and 14). The EDS analysis was accomplished at both 100X and 1000X to determine if there was a significant difference, but none was observed. Only the 100x line scan data are presented. Additionally, samples at 12 mm and 36 mm from the bottom of the Y-block were examined, but no differences were observed, so only the 12 mm data are presented. Both line scans show little variation across the length. In the Mn data, a very small content variation might be observed; however, it is not significant.

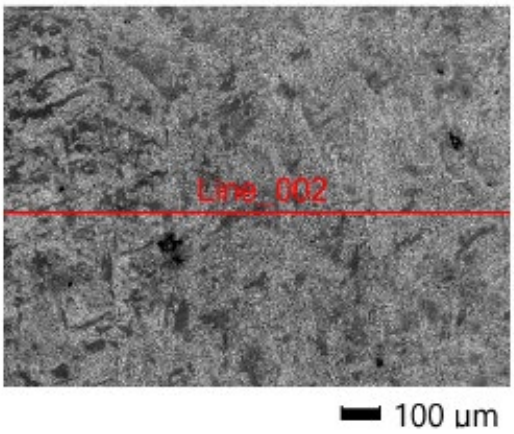

Figure 11. The area where EDS line scan data was measured for QP1 is shown.

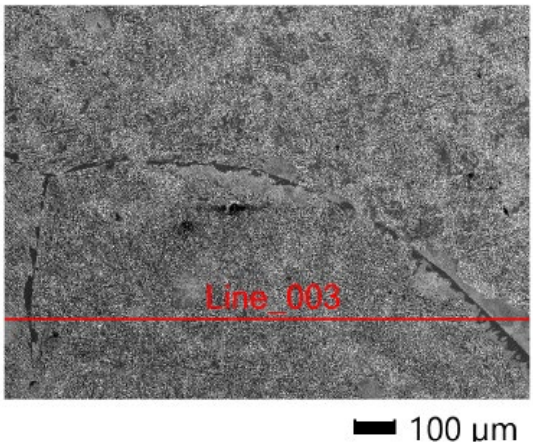

Figure 12. The area at 12mm where EDS line scan data was measured for QP2.

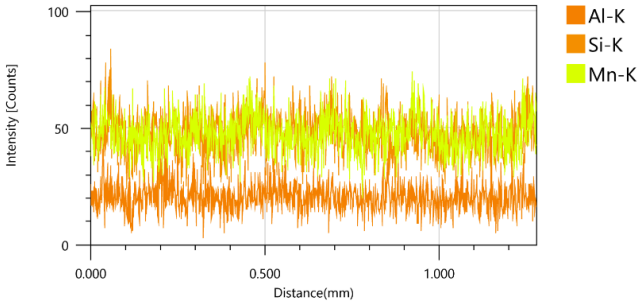

Figure 13. The EDS line scan data for QP1.

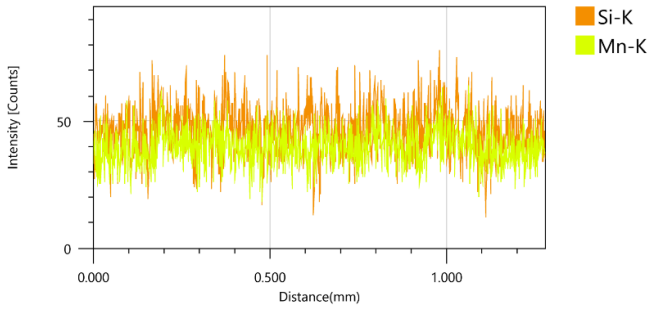

Figure 14. The EDS line scan data for QP2.

The EDS results match the microstructure observations. If Mn or Si segregation had been significant, the authors would have expected to detect areas with very different microstructure. The observed structure was very consistent which also indicated no segregation at the micro scale. Thus, the microsegregation and macrosegregation observations were similar in these alloys in a 25.4 mm thick section. Figure 15 and 16 depict the EDS mapping of elements for QP1 and QP2 alloys respectively. These maps show a relatively even composition across the material.

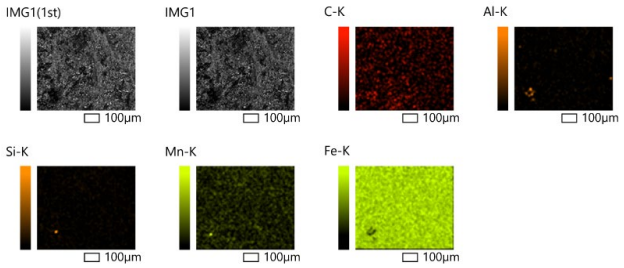

Figure 15. The EDS mapping of element distribution for the QP1 alloy.

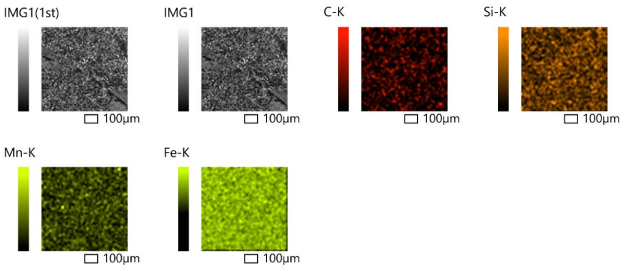

Figure 16. EDS mapping of element distribution for the QP2 alloy.

The results in this work appear to contradict the other research published on segregation in these steels. The reader will remember that according to research by Wang et al. and Hajy Akbary et al., it was observed that there was severe Mn segregation within these types of steel.[11,19] They summarized their research showing that between Mn and C, segregation of Mn has a dominant influence on the microstructure of the Q&P steels.[11,19] Based on these segregation findings, other authors carried out a homogenization step in their experiments.[3,10,17,18]

The sample thickness in this experiment was 25.4 mm thick whereas Wang et al. and Hajy Akbary et al., in their respective studies, did not furnish comprehensive information regarding the original casting details of the samples they used. Instead, they mentioned that the source of their samples were steel mills. Typically, steel mills, cast slabs that are 250-300 mm thick. In these thicker sections, the solidification time is longer leading to more significant segregation.[21] Alloying elements tend to concentrate more in the liquid during solidification. Thus, a longer solidification time leads to more variation in composition across the material. The casting in this work is an order of magnitude smaller. It appears that in this size range that segregation tends to be negligible. Considering the data from this work, there is no requirement for including a homogenizing stage in the heat treatment of these steels in casting up to this section size. Large castings may still require homogenization.

CONCLUSIONS

In this paper, two medium-Mn steels were analyzed for indications of macro and microsegregation. Their microstructures consisted of martensite, retained austenite, and some ferrite. The C, Mn, and Si were consistent across various locations within the Y-block castings. Also, EDS line scans found no significant segregation at the microstructure level.

As per the findings of this analysis, the alloying elements were uniformly distributed throughout the 25.4 mm thick casting. Therefore, it may not be necessary to include a homogenizing stage in the process for castings up to 25.4 mm thick in these steels. This omission has the potential to reduce both the cost and time required in industrial processes.

ACKNOWLEDGEMENTS

The authors would like to thank Jacob Paquette and Demetrios Cortez for their assistance in pouring the castings for these experiments. Their help was instrumental in completing this work.

REFERENCES

1. Wendler, M., Ullrich, C., et al., "Quenching and Partitioning (Q&P) Processing of Fully Austenitic Stainless Steels," *Acta Materialia*, vol. 133, pp. 346–355 (2017).
2. Callister, W.D., "Materials Science and Engineering: An Introduction," Wiley, New York, (2006).
3. Cao, R., Liang, J., Li, F., Li, C. & Zhao, Z., "Intercritical Annealing Processing and a New Type of Quenching and Partitioning Processing, Actualized by Combining Intercritical Quenching and Tempering, for Medium Manganese Lightweight Steel," *Steel Research International*, vol. 91 (1), 1900335 (January 2020).
4. Cheng, Y.Y., Zhao, G., Xu, D.M., Mao, X.P., Bao, S. Q. & Yang, G.W., "Comparative Study on Microstructures and Mechanical Properties of Q&P Steels Prepared with Hot-rolled and Cold-rolled C–Si–Mn Sheets," *Journal of Materials Research and Technology*, vol. 20, pp. 1226–1242 (2022).
5. Zhang, K., Liu, P., Li, W., Ma, F., Guo, Z. & Rong, Y., "Enhancement of the Strenght and Ductility of Martensitic Steels by Carbon," *Materials Science and Engineering: A*, vol. 716, pp. 87–91 (2018).
6. He, B. B., Liu, L. & Huang, M.X., "Room-Temperature Quenching and Partitioning Steel," *Metallurgical and Materials Transactions A*, vol. 49 (8), pp. 3167–3172 (2018).
7. Wang, G.-T., Zhou, Y.-L., Wang, L.-J. & Liu, C.-M., "Study on Microstructures and Properties of Low-Carbon-Steel Heavy Plate Treated by Quenching and Dynamic Partitioning," *Journal of Materials Engineering and Performance*, vol. 31 (2), pp. 1195–1203 (2022).
8. Meng, L., Li, W., Shi, Q., Guo, H., Liang, W. & Lu, H., "Effect of Partitioning Treatment on the Microstructure and Properties of Low-carbon Ferritic Stainless Steel Treated by a Quenching and Partitioning Process," *Materials Science and Engineering: A*, vol. 851, pp. 143658 (2022).
9. Mohapatra, J.N., Dabbiru, S.K. & Balachandran, G., "Development of Ultra-high Strength Steel with a Versatile Range of Properties by Single Stage Quench Partitioning Process," *Transactions of the Indian Institute of Metals*, vol. 76 (7), pp. 1905–1913 (2023).
10. Mohammadi Zahrani, M., Ketabchi, M. & Ranjbarnodeh, E., "Microstructure Development and Mechanical Properties of a C-Mn-Si-Al-Cr Cold Rolled Steel Subjected to Quenching and Partitioning Treatment," *Journal of Materials Research and Technology*, vol. 22, pp. 2806–2818 (2023).
11. Wang, J., Qian, R., Yang, X., Zhong, Y. & Shang, C., "Effect of Segregation on the Microstructure and Properties of a Quenching and Partitioning Steel," *Materials Letters*, vol. 325, pp. 132815 (2022).
12. Gerdemann, F., Speer, J.G. & Matlock, D.K., "Microstructure and Hardness of Steel Grade 9260

Heat-treated by the Quenching and Partitioning (Q&P) Process," *MS&T 2004 Conference Proceedings*, pp. 439–449 (2004).
13. Speer, J.G., Streicher, A.M., Matlock, D.K., Rizzo, F. & Krauss, G., "Quenching and Partitioning: A Fundamentally New Process to Create High Strength TRIP Sheet Microstructures," *Austenite Formation and Decomposition*, pp. 505–522 (2003).
14. Lobo, J.A. & Geiger, G.H., "Thermodynamics of Carbon in Austenite and Fe-Mo Austenite," *Metallurgical Transactions A*, vol. 7 (8), pp. 1359–1364 (1976).
15. Lobo, J.A. & Geiger, G.H., "Thermodynamics and Solubility of Carbon in Ferrite and Ferritic Fe-Mo Alloys," *Metallurgical Transactions A*, vol. 7 (8), pp. 1347–1357 (1976).
16. Speer, J., Matlock, D.K., De Cooman, B.C. & Schroth, J.G., "Carbon Partitioning into Austenite after Martensite Transformation," *Acta Materialia*, vol. 51 (9), pp. 2611–2622 (2003).
17. Ayenampudi, S., Celada-Casero, C., et al., "Microstructural Impact of Si and Ni During High Temperature Quenching and Partitioning Process in Medium-Mn Steels," *Metallurgical and Materials Transactions A*, vol. 52 (4), pp. 1321–1335 (2021).
18. Li, H.Y., Lu, X. W., Wu, X.C., Min, Y. A. & Jin, X.J., "Bainitic Transformation During the Two-step Quenching and Partitioning Process in a Medium Carbon Steel Containing Silicon," *Materials Science and Engineering: A*, vol. 527 (23), pp. 6255–6259 (2010).
19. HajyAkbary, F., Sietsma, J., Petrov, R.H., Miyamoto, G., Furuhara, T. & Santofimia, M.J., "A Quantitative Investigation of the Effect of Mn Segregation on Microstructural Properties of Quenching and Partitioning Steels," *Scripta Materialia*, vol. 137, pp. 27–30 (2017).
20. Gao, P., Li, F., An, K., Zhao, Z., Chu, X. & Cui, H., "Microstructure and Deformation Mechanism of Si-strengthened Intercritically Annealed Quenching and Partitioning Steels," *Materials Characterization*, vol. 191, pp. 112145 (2022).
21. Choudhary, S.K., Ganguly, S., Sengupta, A. & Sharma, V., "Solidification Morphology and Segregation in Continuously Cast Steel Slab," *Journal of Materials Processing Technology*, vol. 243, pp. 312–321 (2017).